This is an *Accepted Manuscript*, which has been through the Royal Society of Chemistry peer review process and has been accepted for publication.

Accepted Manuscripts are published online shortly after acceptance, before technical editing, formatting and proof reading. Using this free service, authors can make their results available to the community, in citable form, before we publish the edited article. We will replace this *Accepted Manuscript* with the edited and formatted *Advance Article* as soon as it is available.
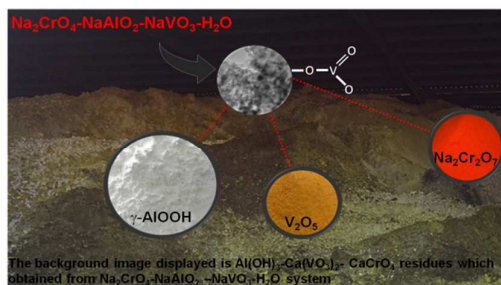
You can find more information about *Accepted Manuscripts* in the **Information for Authors**.

A table of contents entry

Source reduction of hazardous Cr^{6+} containing wastes has the significance to the cleaner production of chromate and environment protection.

The vanadate adsorption on a mesoporous boehmite and its cleaner production application of chromate

Ping Li[a,b], Sili Zheng† [a,b], Penghui Qing [a,b], Yongan Chen [a,b], Lei Tian [a,b], Xiaodan Zheng [a,b], Yi Zhang [a,b]
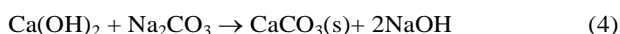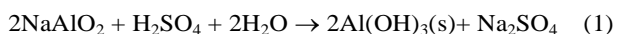
A mesoporous boehmite (γ-AlOOH) synthesis and vanadate (V(V)) ions adsorption and desorption on the mesoporous γ-AlOOH were investigated. The synthesis and adsorption studies showed that the mesoporous γ-AlOOH with BET surface of 442 $m^2 \cdot g^{-1}$ and pore size of 2.75 nm possessed a maximum V(V) ions adsorption capacity of 3.28 $mmol \cdot g^{-1}$. The adsorption mechanisms results showed that the mesoporous γ-AlOOH liberated surface hydroxyls to form coordinatively unsaturated Al^{VI} centres to adsorb V(V) ions which connected oxygen of the coordinatively unsaturated Al^{VI} centres with mono-oxo, V=O terminal double bonds. The desorption studies showed that the V(V) ions could be desorbed by $NH_3 \cdot H_2O$ easily. In the cleaner production application of chromate, the mesoporous γ-AlOOH was synthesized in the Na_2CrO_4–$NaAlO_2$–$NaVO_3$–H_2O solutions of the chromate production and then in situ adsorbed the V(V) ions. The results showed that the V(V) ions were removed effectively, so that the highly carcinogenic $CaCrO_4$ containing $Ca(VO_3)_2$ residue which obtained by typical process of chromate production was eliminated. Therefore, green separation of V(V) ions to reduce waste pollution in ensuring economy and feasibility premise could be expected.

1.Introduction

Vanadium (V) and chromium (Cr) as the important alloying elements are widely associated in the chromite, bauxite, vanadium titano-magnetite, and molybdentite, etc. which are the main raw materials of Cr, aluminum (Al), V and molybdenum (Mo) metallurgy.[1, 2] On the other hand, V and Cr are the main dangerous heavy metal pollutants. Therefore, Cleaner production of V and Cr to prevent pollution are important for the related metallurgical process and environment protection.

Many environmental friendly approaches have been practiced in separating V and Cr, such as chemical precipitation, biological treatment, membrane filtration, ion exchange, extraction, and adsorption.[3] At present, the liquid–liquid extraction and ion exchange methods are mainly used to separate V in the V and Mo metallurgy.[4,5] For the inexpensive metals, such as Al and Cr, the chemical precipitation method is preferred.[6] However, these methods also produce new industrial waste, notably the waste of Cr metallurgy (chromate production). As a typical chromate production process, the Na_2CrO_4–$NaAlO_2$–$NaVO_3$–H_2O solutions are produced after roasting the chromite with Na_2CO_3. In order to obtain Na_2CrO_4–H_2O solutions to prepare sodium dichromate ($Na_2Cr_2O_7 \cdot 2H_2O$) product, separation reactions of Al and V are as follows:

$$2NaAlO_2 + H_2SO_4 + 2H_2O \rightarrow 2Al(OH)_3(s) + Na_2SO_4 \quad (1)$$

$$2NaVO_3 + Ca(OH)_2 \rightarrow Ca(VO_3)_2(s) + 2NaOH \quad (2)$$

$$Na_2CrO_4 + Ca(OH)_2 \rightarrow CaCrO_4(s) + 2NaOH \quad (3)$$

$$Ca(OH)_2 + Na_2CO_3 \rightarrow CaCO_3(s) + 2NaOH \quad (4)$$

The Al(III) and V(V) are gradually removed due to low solubilities of $Al(OH)_3$ (Equation 1) and $Ca(VO_3)_2$ (Equation 2). In addition, a highly carcinogenic $CaCrO_4$ is generated at the same time (Equation 3).[7] Na_2CO_3 is also added to remove excessive soluble Ca^{2+} (Equation 4). The separation method produces Cr(VI) containing $Al(OH)_3$ residue and $CaCrO_4$ containing $Ca(VO_3)_2$ residue, resulting in serious environment pollution and waste of resources. It is estimated that in the chromate production, each 1000 kg of $Na_2Cr_2O_7 \cdot 2H_2O$ product will be accompanied by approximately 200kg of $Al(OH)_3$ and 50-100 kg of $Ca(VO_3)_2$ which contained about 5 kg of $CaCrO_4$.[8] Such "taking stop gap measures" method is obviously contrary to the development trend of green separation, but still popular because of its advantages of high feasibility and low cost. Reducing the wastes from the source in ensuring economy and feasibility premise has the vital significance to the cleaner production of chromate.

Boehmite (γ-AlOOH) exhibits a lamellar structure, in which the A1(III) ions occupy some of the octahedral holes of the close-packed O^{2-} array and possess the sole octahedral coordination (Al^{VI}), thus yielding coordinatively unsaturated Al^{VI} centres.[9] The γ-AlOOH is inclined to adsorb ions due to its coordinatively unsaturated Al^{VI} centres on the surface, which allows it to be one of the important adsorbent materials. In order to obtain more coordinatively unsaturated Al^{VI} centres, the γ-AlOOH with various nanostructures and morphologies, such as nanostructures, mesoporous structures, hierarchical flower-like and other morphologies, has been prepared to adsorb heavy metal ions. For example, the coordinatively unsaturated Al^{VI} centres were produced by liberating surface hydroxyls from H-bonding on the calcined nanosized γ-AlOOH to adsorb As^{3+}.[10] The γ-AlOOH nanorods with (100) facet exposure were prepared; and the (100) facet with more unsaturated Al^{VI} centres exhibited a high adsorption ability to $Cr_2O_7^{2-}$.[11] The hierarchical flower-like γ-AlOOH with a large BET area was prepared to adsorb Pb^{2+} and Hg^+.[12] However, synthesis of the mesoporous γ-AlOOH and V(V) ions adsorption behavior onto the mesoporous γ-AlOOH have been rarely studied.

This study thus aimed at synthesizing the mesoporous γ-AlOOH based on reacting $NaAlO_2$ solutions with H_2SO_4 firstly, and then adsorbing V(V) ions onto the mesoporous γ-AlOOH. Synthesis of the mesoporous γ-AlOOH was studied, key factors and mechanism that influenced the V(V) ions adsorption behavior from aqueous solutions onto the mesoporous γ-AlOOH were also investigated. The V(V) ions desorption behavior from the mesoporous γ-AlOOH and competitive adsorption and desorption behavior of V(V) and Cr(VI) ions were preliminary described. The related clear production application in the Na_2CrO_4–$NaAlO_2$–$NaVO_3$–H_2O solutions system of chromate production was discussed. Therefore, the following purposes are realized: i) V(V) is separated without introducing Ca^{2+} so that the $CaCrO_4$ containing $Ca(VO_3)_2$ residue is eliminated; ii) easier integrated utilization of V(V) and Al(III): high added value of V_2O_5 and mesoporous γ-AlOOH can be easily obtained by V(V) ions containing mesoporous γ-AlOOH. At last, green separation of V(V) and Cr(VI) to reduce resources of waste in ensuring economy and feasibility premise can be expected.

2. Experimental

All chemicals were analytical grade reagents and used as received without further purification. For a typical synthesis of mesoporous γ-AlOOH, 55 mL 3.6 mol· L^{-1} H_2SO_4 was added into 400 mL 48 g· L^{-1} $NaAlO_2$ at 60 °C for 20 min, and the pH values of the solution were controlled by the amount of H_2SO_4. The mesoporous γ-AlOOH was then centrifuged and washed with distilled water till not any SO_4^{2-} could be detected, filtered and vacuum-dried at 60 °C for 24 h.

For the adsorption of V(V), a known amount of mesoporous γ-AlOOH and $NaVO_3$· $2H_2O$ solution were placed in a 250 mL Teflon bottle and the pH adjusted to the desired value with the dropwise addition of $NaOH/H_2SO_4$. The suspension solution was agitated at constant speed in a shaking machine at certain temperature over a period of time and filtered. The filtrate was then analyzed for residual V(V) ions. The experimental parameters studied were contact time (0.25-6 h) with varying $NaVO_3$·$2H_2O$ solution concentration (5-50 g· L^{-1}), at different temperature (20-90 °C) with varying pH (1-12), and effect of co-existing ions. The mesoporous γ-AlOOH concentration in solution was therefore 40 g· L^{-1}. All the adsorption experiments were conducted in triplicate, and the mean values were reported.

For the desorption of V(V) , the mesoporous γ-AlOOH after V(V) adsorption was separated from the $NaVO_3$·$2H_2O$ aqueous solution and washed with deionized water to remove unadsorbed V(V). Then 50 g mesoporous γ-AlOOH after V(V) adsorption was added to 200 mL 50 g· L^{-1} NH_3·H_2O solution to form suspension solution. The suspension solution was shaken at 90 °C for 3 h. The mesoporous γ-AlOOH after V(V) binding desorption was then centrifuged and washed with distilled water, filtered and vacuum-dried at 60 °C for 24 h.

The phases and structure of the mesoporous γ-AlOOH before and after V(V) adsorption were analyzed by X-ray diffraction (XRD), Fouier transform infrared spectroscopy (FT-IR). The XRD analysis was carried out with a Rigaku diffractometer using CuK*a* radiation. The FT-IR spectra were recorded by a SpectraGXFT-IR Spectrometer in KBr pellets (0.002 g sample and 0.2 g KBr) with the scan number set to 8 and the resolution set to 4 cm⁻¹. The morphological

characterization of the mesoporous γ-AlOOH was performed by transmission electron microscopy (TEM) on a JEOL JEM 2100 (UHR) instrument operated at an acceleration voltage of 200 kV. BET surface areas of the mesoporous γ-AlOOH were measured by using Quantachrome Autosorb Automated Gas Sorption System (Quantachrome Corporation, USA) by adsorption of nitrogen at -196 °C on 200 mg sample previously degassed at 200 °C for 2 h under high vacuum atmosphere. The XPS data of the mesoporous γ-AlOOH before and after V(V) adsorption were obtained with an ESCALab220i-XL electron spectrometer from VG Scientific using 300 W AlKα radiation.

3. Results and discussion

3.1 Synthesis of γ-AlOOH

Figure 1 shows the typical XRD pattern and TEM image of the γ-AlOOH synthesized at pH 7. As shown in XRD pattern of the Fig. 1a, all peaks of the synthesized γ-AlOOH could be clearly indexed as a boehmite phase, which was consisted with the reported data, for AlO(OH) (JCPDS 21-1307).[13] The XRD pattern also showed a broadened (002) γ-AlOOH peaks and a relatively low diffraction intensity, suggesting a small crystallite size (74± 5 nm) in nanometer scale.[14] TEM image of the γ-AlOOH exhibited irregular agglomerates. The agglomerates could be the agglomerates of the stack of flakes (Fig. 1b, inset).
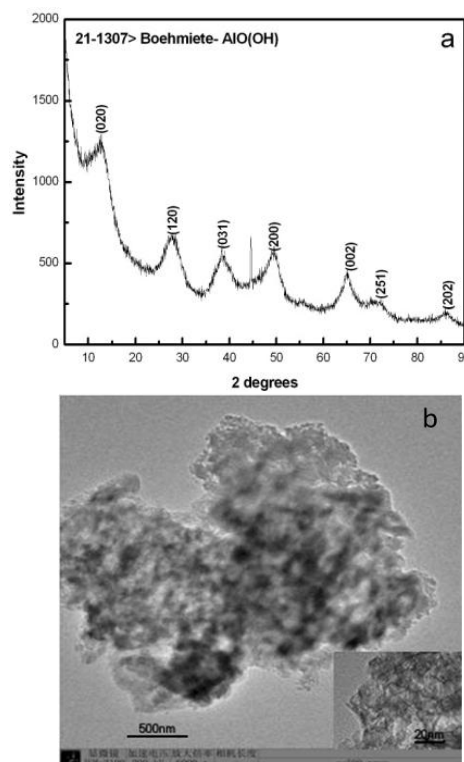

Figure 1 (a) XRD pattern and (b) TEM image of the synthesized γ-AlOOH.

To determine the BET surface of the γ-AlOOH, their N₂ adsorption and desorption isotherms were measured at -196 °C. Figure 2 shows the plots of N₂ adsorption and desorption isotherms

and pore size distributions, respectively. For mesoporous and macroporous materials, the standard BET analysis is performed at a pressure range of $0.05 < P/P_0 < 0.35$ (For the obtained linear equation, the Y-intercept must be positive to yield a meaningful value of the C value, as shown in the inset of Fig. 2a).[15,16] The resultant BET surface was 442 m[2]· g^{-1} for γ-AlOOH. The isotherms and hysteresis loops of synthesized γ-AlOOH belong to the typical type H4 loop (based on the IUPAC classification), indicating containing slit-shaped mesopores and microporosity that are associated with capillary condensation.[17] As illustrated in Fig. 2b, the γ-AlOOH displayed a mean pore diameter of 2.75 nm calculated from the desorption branch of the isotherm (BJH method). The total pore volume determined at $P/P_0 = 0.993$ reached 0.342.

Overall, the XRD and BET analysis indicate that the synthetic sample is the mesoporous γ-AlOOH with BET surface of 442 m[2] g^{-1} and pore size of 2.75 nm.

recognized by its diffraction peaks at 2θ= 18.7° for (001), 20.4° for (020), 40.7° for (201). On the basis of the pH-dependent experiments, it can be seen that an acidic condition and a neutral condition (pH≤ 7) are vital for the γ-AlOOH formation, while the α-Al(OH)₃ formation is favored under alkaline conditions.

Figure 3 XRD patterns of the samples at different pH values.

Figure 4 Adsorption of V(V) ions onto the mesoporous γ-AlOOH as a function of (a) initial pH, (b) NaVO₃· 2H₂O addition, (c) temperature, (d) time.
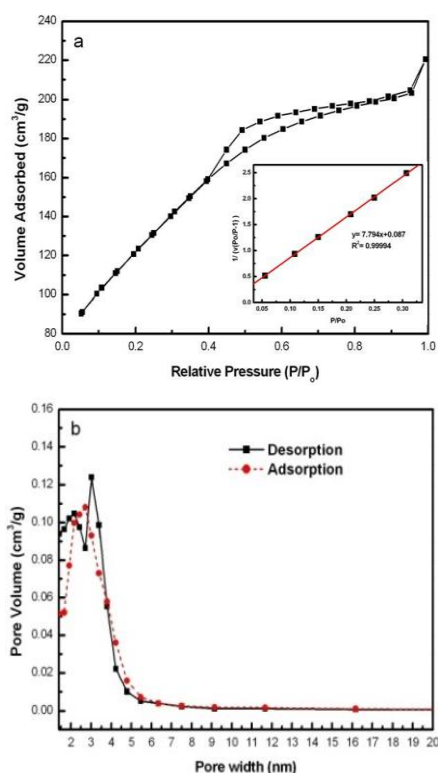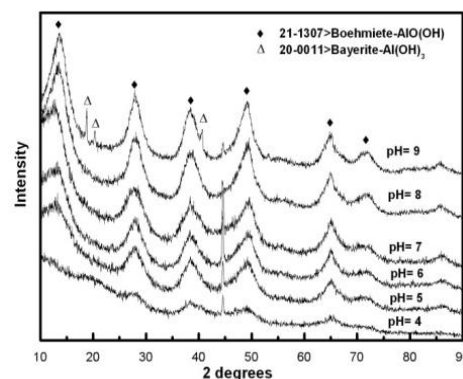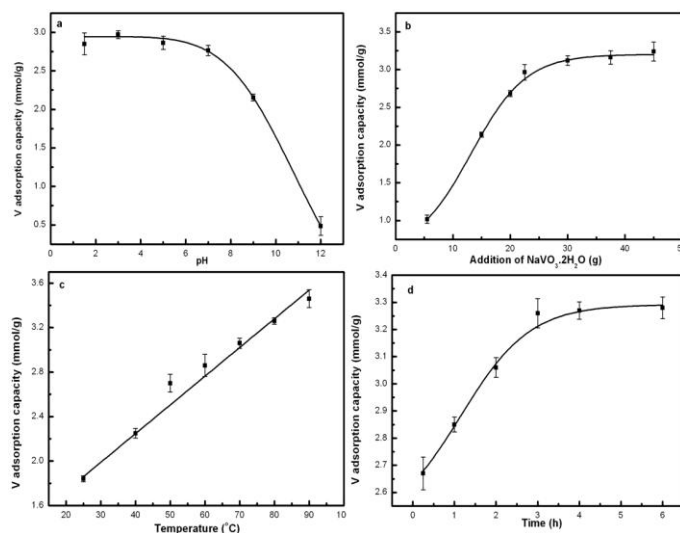

Figure 2 (a) Nitrogen adsorption-desorption isotherms of synthesized γ-AlOOH. The inset in (a) is six-point BET plots in the selected pressure ranges for N₂ on γ-AlOOH. (b) Pore size distribution profiles of γ-AlOOH derived by using BJH method.

To investigate the crucial synthesized conditions of the mesoporous γ-AlOOH, pH-dependent experiments were conducted to reveal the formation process. XRD were employed to monitor the crystalline structure of the samples collected at different pH. Figure 3 shows the XRD patterns of the samples synthesized at different pH values. As shown in Fig. 3, at pH≤ 8, the boemhite phase was identified by the characteristic diffraction peaks of γ-AlOOH at 2θ= 13.2° for (020), 28.1° for (120), 38.6° for (031), 49.7° for (200), and 65.0° for (002). By increasing the pH value to 9, a small portion of the bayerite (α-Al(OH)₃) phase was

3.2 Adsorption behavior

In adsorption processes, the adsorption of metal ions on mineral surfaces can be reduced or increased by the initial pH values of the solution. Vanadium is an active metal that exists in + 3, + 4 and + 5 oxidation states, and twelve vanadium species can coexist in solution. These can be categorized as cationic species [VO₂⁺] which exists mainly at lower pH ≤2, and anionic species (decavanadate species and other mono or polyvanadate species), respectively.[18] Some experiments were carried out to examine the influence of initial pH on the adsorption of V(V) ions with 50 g· L^{-1} NaVO₃· 2H₂O, 40 g· L^{-1} mesoporous γ-AlOOH, at 60 °C for 3 h. The initial pH of V(V) ions solutions was adjusted from 1 to 12 with H₂SO₄ and NaOH solutions. The results obtained are shown in Fig. 4a. The V(V)

ions adsorption followed a typical metal anion adsorption behavior onto the mesoporous γ-AlOOH, where negligible adsorption occurred at a high pH and a sharp decrease in adsorption in alkaline media. The decrease in V(V) ions adsorption at high pH may be due to competition between OH^- and V(V) ions for available surface sites.[19] At pH ≤7, high and stable adsorption of V(V) ions onto the mesoporous γ-AlOOH were kept constant. So, it can be expected that the maximum adsorption of V(V) ions can occur at the suitable acid or neutral pH value.

Assessment of the effect of initial concentration on the V(V) ions adsorption onto the mesoporous γ-AlOOH was carried out by varying the additive amount of $NaVO_3 \cdot 2H_2O$ (5 g· L^{-1} to 50 g· L^{-1}) at pH 7, 60 °C for 3 h. The results of the adsorption of V(V) ions are shown in Fig. 4b. It was found that the adsorption of V(V) ions onto the mesoporous γ-AlOOH was strongly dependent on initial V(V) ions concentration. The removal of V(V) ions from aqueous solutions onto the mesoporous γ-AlOOH was found to increase from 1.0 mmol· g^{-1} to 3.0 mmol· g^{-1} with the increase of V(V) ions concentration. When the $NaVO_3 \cdot 2H_2O$ concentration was less than 25 g· L^{-1}, the V(V) ions adsorption capacity of the mesoporous γ-AlOOH linearly increased, and the maximum up to 3 mmol· g^{-1}; after that, higher than that of 25 g· L^{-1}, the V(V) ions absorption capacity of mesoporous γ-AlOOH increased slightly. Such adsorption behavior at higher concentrations may also result from a decrease in the driving force of the concentration gradient.[20]

The effect of temperature in the adsorption of V(V) ions onto the mesoporous γ-AlOOH was also investigated. The temperature was varied from 20 to 90 °C at pH 7, 3 h and $NaVO_3 \cdot 2H_2O$ concentration of 50 g· L^{-1}. It was observed that the adsorption of V(V) ions increased with the increase of temperature (Fig. 4c). Note that there was a better adsorption at higher temperature. The increase in amount of vanadium adsorbed with an increase in temperature is provoked by more mobility of the ionic species present in the $NaVO_3 \cdot 2H_2O$ solution, with acceleration of some originally slow adsorption steps or by creation of some new active sites on the mesoporous γ-AlOOH surface.

The adsorption processes as a function of time to determine the point of equilibrium were studied from adsorption experiments of V(V) ions onto the mesoporous γ-AlOOH. These experiments were carried out at an initial pH 7 without pH adjustment in the presence of 50 g·L^{-1} $NaVO_3 \cdot 2H_2O$ at 60 °C. The results were shown in Fig. 4d, where it was clear that adsorption of V(V) ions onto the mesoporous γ-AlOOH was quick and after 3 h the complete adsorption equilibrium was obtained. The amount of V(V) ions removed reached a maximum of 3.28 mmol· g^{-1}. No further adsorption above the quantity obtained in 3 h was obtained by placing the mesoporous γ-AlOOH in contact with $NaVO_3 \cdot 2H_2O$ solutions for 6 h of shaking time.

3.3 Desorption behavior

A desorption studies indicate that the V(V) ions that have been adsorbed on mesoporous γ-AlOOH can be easily desorbed by using 50 g· L^{-1} $NH_3 \cdot H_2O$ solution at 90 °C for 3 h. Very high

desorption rate (99%) showed that adsorption of V(V) ions on mesoporous γ-AlOOH was reversible. Similar observations were reported from the V(V) ions adsorption onto Fe(III)/Cr(III) hydroxide and Zr(IV)-impregnated collagen fiber.[21,22]

3.4 Adsorption kinetics and equilibrium

To understand the dynamics of the V(V) ions adsorption process, the V(V) ions adsorption kinetic data were analysed using two mass transfer models: a pseudo-first-order equation and a pseudo-second-order equation.

The pseudo-first-order equation is given as:

$$\ln(a_m - a) = \ln a_m - k_1 t \qquad (1);$$

The pseudo-second-order equation is expressed as:

$$\frac{t}{a} = \frac{1}{k_2 a_m^2} + \frac{1}{a_m} t \qquad (2);$$

The adsorption kinetic model parameters obtained from the above plots are given in Table 1. From this table it is suggested that a pseudo-second-order model is more suitable to describe the adsorption kinetics because of the values of correlation coefficient R^2 (>0.999) for this model. Furthermore, the values of adsorption capacity as determined by the pseudo-second-order model are closer to the calculated experimental data. Therefore, it has been concluded that the pseudo-second-order model is appropriate to represent the adsorption kinetics of V(V) ions by the mesoporous γ-AlOOH. It indicates that the adsorption mechanism of V(V) ions onto the mesoporous γ-AlOOH might be a chemisorptions process.

The Langmuir model and Freundlich model are the most frequently employed models to describe experimental data of adsorption isotherms. The models can be described by the following equation:[23]

$$a = K C_e^{1/n} \quad \text{Freundlich model} \qquad (3);$$

$$a = \frac{a_m b C_e}{(1 + b C_e)} \quad \text{Langmuir model} \qquad (4);$$

Where

C_e and a represent the V(V) ions concentration in solutions and the mesoporous γ-AlOOH at equilibrium, respectively,

K is a constant related to the adsorption capacity,

a_m is the maximum adsorption capacity,

b and n are constants related to the energy of adsorption.

Table 2 lists the values of both the Freundlich and Langmuir parameters from the linearized versions of the two isotherms with their corresponding correlation coefficients (R_1^2). The Freundlich parameters were evaluated with the help of slope and intercept of the linear plot, $1/n$ and log K were found to be 0.578 and 2.112, respectively. The values of $1/n$ between $0.1 < 1/n < 1$ represent good adsorption of V(V) ions. Langmuir equation is probably the most widely applied model for isotherm adsorption, it considers that the adsorption energy of each molecule is the same, independently of the surface of material, the adsorption takes place only on some sites and there are on interaction between the molecules. The Langmuir parameters were a_m = 3.61 mmol· g^{-1}, and b = 0.156. The values of the correlation coefficient R_1^2 demonstrates that the data are best fitted to Langmuir than Freundlich equation.

Table 1 Adsorption rate constant obtained from pseudo-first-order model and pseudo-second-order model of V(V) ions on mesoporous γ-AlOOH.
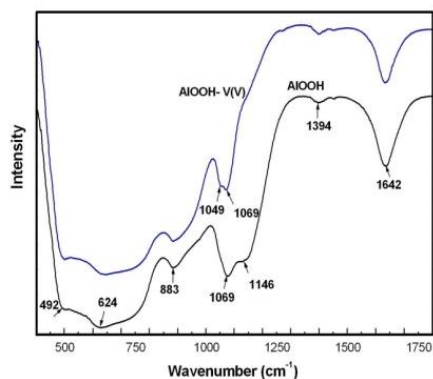
Initial NaVO$_3$ 2H$_2$O conc.(g·L^{-1})	a$_{mexp}$ (mmol·g^{-1})	Pseudo-first-order			Pseudo-second-order		
		K$_1$ (h^{-1})	a$_m$(mmol·g^{-1})	R^2	K$_2$(g(mmol·h)$^{-1}$)	a$_m$(mmol·g^{-1})	R^2
50	3.28	1.198	4.126	0.913	2.488	3.606	0.999

Table 2 Langmuir and Freundlich parameters for V(V) ions adsorption onto mesoporous γ-AlOOH at pH of 7 and V(V) ions concentration of from 31.65 mmol· L^{-1} to 316.5 mmol· L^{-1} (NaVO$_3$·2H$_2$O concentration from 5 g· L^{-1} to 50 g· L^{-1}).

Media	Freundlich parameters			Langmuir parameters		
	1/n	log K	R$_1^2$	a$_m$(mmol·g^{-1})	b(L·mmol^{-1})	R$_1^2$
γ-AlOOH	0.578	2.112	0.958	3.61	0.156	0.988

3.5 Adsorption mechanism

Figure 5 FT-IR spectra of the mesoporous γ-AlOOH (AlOOH) and the mesoporous γ-AlOOH after V(V) adsorption (AlOOH-V) at pH 7, 60 ^{o}C, 3 h.

The vibration models associated with the stretching and bending motions of M-OH functional groups are sensitive to the presence of adsorbed anions, which can be detected by FT-IR spectroscopy. FT-IR spectra of the mesoporous γ-AlOOH (AlOOH) and the mesoporous γ-AlOOH after V(V) ions adsorption (AlOOH-V) in NaVO$_3$·2H$_2$O solutions at pH 7 for 3 h are shown in Figure 5. In the FT-IR spectrum of AlOOH, Bands at 1642 cm^{-1} were characteristics of adsorbed water. Unidentate carbonate species were found at 1394 cm^{-1}. The four absorption bands at around 1146, 1069 and 883, 624, and 492 cm^{-1} were assigned to the O-H bending, (HO)-Al=O asymmetric stretching, (OH)-Al=O angle bending, and O=Al-(OH) angle deformation vibrations, respectively.[24] Unlike the above results, it was clear that the Al-OH bending bands (1146 cm^{-1}) disappeared in the FT-IR spectrum of the AlOOH-V, while a new band, corresponding to a V=O terminal bond, appeared at 1049 cm^{-1}.[25] An isolated tetrahedral vanadium oxide species possess a single, mono-oxo V=O terminal bond (band at 1016-1040 cm^{-1}) and three V-O-V bonds (band at 840-940 cm^{-1}).[26,27] Therefore, the shoulder of AlOOH-V present in the FT-IR spectrum at 1049 cm^{-1} is most likely due to mono-

oxo, V=O terminal double bonds within VO$_4$ units of slightly different asymmetries.
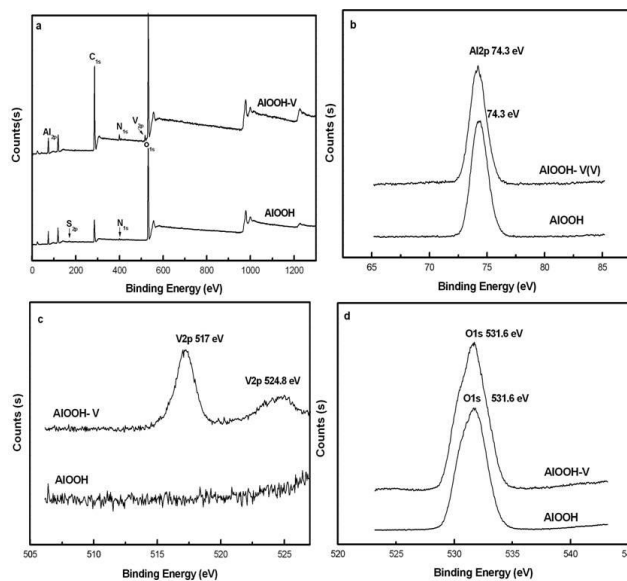
Figure 6 XPS spectra for (a) the mesoporous γ-AlOOH (AlOOH) and the mesoporous γ-AlOOH after V(V) adsorption (AlOOH-V), (b) Al 2p, (c) V 2p, (d) O 1s.

X-ray photoelectron spectroscopy is widely used for studies of surface chemistry because it provides a range of useful information depths, reasonable quantification, and chemically specific information for each element detected through chemical shifts.[28] To investigate the surface states of the mesoporous γ-AlOOH after V(V) ions adsorption, a typical scan of the mesoporous γ-AlOOH (AlOOH) and the mesoporous γ-AlOOH after V(V) ions adsorption (AlOOH-V) provide XPS spectra with clearly resolved Al2p, V2p and O1s peaks (Fig. 6). As shown in Fig. 6c, The V2p XPS spectra indicated that V(V) ions adsorption occurred on the surface of mesoporous γ-AlOOH. The binding energy of Al2p at 74.3 eV (Fig. 6b) and the peak shape

indicated that the dominating chemical state of Al atoms in the mesoporous γ-AlOOH was Al(III).[29] The Al2p spectrum of γ-AlOOH after V(V) ions adsorption showed little change, indicating that the chemical state of Al atoms did not changed after V(V) ions adsorption. The O 1s peaks are composed of subpeaks with peak energies $\approx$530.1–530.3, $\approx$531.5–532.0, and $\approx$532.8–533.4 eV which are designated as surface O^{2-} and OH^- groups and as free H_2O, respectively.[30] Figure 6d showed that the O1s spectra of AlOOH and AlOOH-V were possibly composed of overlapped peaks of oxygen (O^{2-}) and hydroxyl (OH^-). All of the O1s spectra were fitted using a Gaussian: Lorentzian peak shape, [31] and satisfactory fitting results were obtained as shown in Fig. 7 and Table 3.
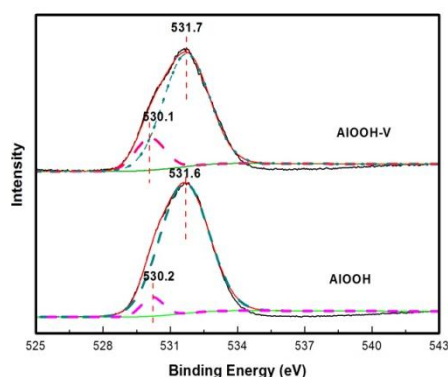

Figure 7 O 1s spectra of for (a) the mesoporous γ-AlOOH (AlOOH) and the mesoporous γ-AlOOH after V(V) adsorption (AlOOH-V). The dotted curves represent photo peak contribution from O^{2-} and OH^-. The peak at the lower binding energy is oxygen (O^{2-}) and the peak at the higher binding energy is OH^-.

Table 3 O 1s peak parameters for different samples.

Sample	Peak	B.E. (eV)	Fwhm (eV)	Percent (%)
AlOOH	O^{2-}	530.2	1.14	6.1
	OH^-	531.6	2.57	93.9
	H_2O	—	—	—
AlOOH-V	O^{2-}	530.1	1.56	15.5
	OH^-	531.7	2.41	84.5
	H_2O	—	—	—

The OH^- was the most abundant (93.9% and 84.5%) followed by O^{2-} (6.1% and 15.5%) in the AlOOH and AlOOH-V. The OH^- content decrease and the O^{2-} increase during the V(V) ions adsorption onto the mesoporous γ-AlOOH are observed, which is similar to liberating surface hydroxyls from H-bonding on the calcined nanosized γ-AlOOH to adsorb As^{3+}.[9] Therefore, the possible adsorption mechanism is that the more coordinatively unsaturated Al^{VI} centres are imposed from the mesoporous γ-AlOOH surface to adsorb vanadate ions, and the vanadate ions are adsorbed onto oxygen of the coordinatively unsaturated Al^{VI} centres directly.

Table 4 Data regarding atomic ratios collected from XPS spectra of different samples.

Atomic ratio %	Al	V	O	S
AlOOH	29.37	—	69.99	0.64
AlOOH-V	25.24	1.07	73.69	—

To further clarify the possibilities, the atomic ratio of Al, O, S and V on the surface of AlOOH and AlOOH-V are summarized in Table 4. The surface of AlOOH contained 29.37% Al, 0% V and 69.99% O, whereas the surface of AlOOH-V contained 25.24% Al, 1.07% V and 73.69% O; the relative Al, V and O surface atomic ratio of AlOOH and AlOOH-V were 1: 0: 2.38 and 1: 0.042: 2.92, respectively, thus offering further confirmation of the inference that O^{2-} content increase appeared to a consistency with the increase of V(V) ions adsorption onto the mesoporous γ-AlOOH. In addition, The S content on the mesoporous γ-AlOOH surface decreased from 0.64% to 0 during the V(V) adsorption onto the mesoporous γ-AlOOH. Generally, SO_4^{2-} may absorb on the solid surface as an out- sphere (H^- bonded) complex or an inner- sphere complex on metal (hydro) oxide surfaces,[32] Only outer-sphere SO_4^{2-} complex are present at the neutral pH value in this study. The outer-sphere SO_4^{2-} complex disappeared after V(V) binding adsorption, implying that V(V) ions had better bonding adsorption abilities on the surface of the mesoporous γ-AlOOH.

The above FT-IR and XPS results showed that the mesoporous γ-AlOOH liberated surface hydroxyls to form coordinatively unsaturated Al^{VI} centres to adsorb vanadate ions, and surface of the mesoporous γ-AlOOH were mainly covered with the monodentate vanadate complexes which connected oxygen of the coordinatively unsaturated Al^{VI} centres with mono-oxo, V=O terminal double bonds.

3.6 Cleaner production application in Na_2CrO_4-$NaAlO_2$-$NaVO_3$-H_2O solutions system

The typical contents of Na_2CrO_4-$NaAlO_2$-$NaVO_3$-H_2O solutions system are as follows: Na_2CrO_4: 250-300 $g \cdot L^{-1}$, $NaAlO_2$: 25-30 $g \cdot L^{-1}$, $NaVO_3$: 1.5-4.0 $g \cdot L^{-1}$. In order to remove Al(III) and V(V), the mesoporous γ-AlOOH was prepared by adding H_2SO_4, and then adsorbed V(V) ions in the Na_2CrO_4-$NaAlO_2$-$NaVO_3$-H_2O solutions. The H_2SO_4 was used to prepare the mesoporous γ-AlOOH because it was not only similar to the typical process, but essential for the subsequent production of $Na_2Cr_2O_7 \cdot 2H_2O$ and CrO_3 products. It has rarely been studied that reacting $NaAlO_2$ solutions with H_2SO_4 to prepare the mesoporous γ-AlOOH; however, characteristics of the Na_2CrO_4–$NaAlO_2$–$NaVO_3$–H_2O solutions, such as low concentration of $NaAlO_2$, adjustable pH values and temperature, are similar to requirements of above synthetic method of mesoporous γ-AlOOH.

**Table 5** Removal rates of V(V) and Al(III) of Na_2CrO_4-$NaAlO_2$-$NaVO_3$-H_2O system.

Na_2CrO_4-$NaAlO_2$-$NaVO_3$ aqueous solutions(g· L^{-1})			Na_2CrO_4-H_2O solutions(g· L^{-1})			Removal rate (%)	
Na_2CrO_4	$NaAlO_2$	$NaVO_3$	Na_2CrO_4	$NaAlO_2$	$NaVO_3$	V(V)	Al(III)
360	26.2	2.8	360	—	0.5	82.1	100
360	26.2	2.7	360	—	0.4	85.2	100
304	23.2	2.9	304	—	0.6	79.3	100
283	32.2	2.6	283	—	0.3	86.0	100
256	19.9	3.9	256	—	0.7	82.0	100
250	15.8	2.9	250	—	0.5	82.8	100
180	10.5	2.0	180	—	0.4	80.0	100

Therefore, the mesoporous γ-AlOOH was prepared by controlling conditions in accordance with the synthetic method of experimental description, for example, pH≤ 7, temperature at about 60 °C, lower adding speed of H_2SO_4 solution, etc., and then in situ adsorbed vanadate ions at 3h. After that, the prepared mesoporous γ-AlOOH suspension solutions were filtered. The filter cake, which was called V(V) containing mesoporous γ-AlOOH, was washed by water to decrease Na_2CrO_4 loss by entrainment. The filtrate was then analyzed for residual vanadate ions.

Table 5 shows the removal rates of V(V) and Al(III) of Na_2CrO_4–$NaAlO_2$–$NaVO_3$–H_2O solutions system after adopting the method. From the table, the contents of $NaAlO_2$ and $NaVO_3$ decreased from approximately 10.5-32.2 g· L^{-1} and 2.0-3.9 g· L^{-1} to 0 and 0.3-0.7 g· L^{-1}, respectively. The removal rates of Al(III) and V(V) reached 100% and 79.3-86%, respectively. In the typical process, Al(III) and V(V) of Na_2CrO_4–$NaAlO_2$–$NaVO_3$–H_2O solutions system were removed by adding H_2SO_4 and ten times amount of $CaCO_3$, and then the removal rates were approximately 100% and 85-90 %, respectively.[33,34] Hence, such method can meet the needs combining with the product requirements and removal rates of Al(III) and V(V) of typical process.

In addition, competitive adsorption and desorption of V(V) and Cr(VI) onto the mesoporous γ-AlOOH are also preliminary investigated. The V(V) and Cr(VI) contents of V(V) containing mesoporous γ-AlOOH were 1.17 mmol· g^{-1} and 0.12 mmol· g^{-1}, respectively. Such Cr(VI) content of mesoporous γ-AlOOH was even lower than Cr(VI) content of the $Al(OH)_3$ residue which obtained by the typical process. Gel performance of the $Al(OH)_3$ probably results in Cr(VI) loss (0.5-1%) by entrainment. The V(V) and Cr(VI) of mesoporous γ-AlOOH were desorbed by the 50 g· L^{-1} NH_3·H_2O solutions, and the removal rates of V(V) and Cr(VI) reached 95% and 100%, respectively. Similar with Zr (IV)- impregnated collagen fiber adsorbent, the mesoporous γ-AlOOH had also high adsorption selectivity to V(V) in the mixture solutions of V(V) and Cr(VI). Through the research of cleaner production application, it is

expected to form the following principal flow sheet of V(V) and Al(III) separation in the Na_2CrO_4–$NaAlO_2$–$NaVO_3$–H_2O solutions system of the chromate production (Scheme 1).
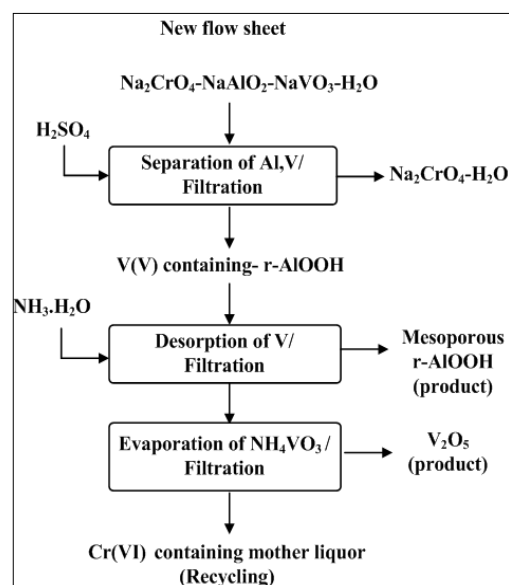
Scheme 1 Principal flow sheet of separation of V(V) and Al(III) in the Na_2CrO_4-$NaAlO_2$-$NaVO_3$-H_2O solutions system of chromate production.

To sum up, the Al(III) and V(V) were removed effectively by synthesizing the mesoporous γ-AlOOH and in situ vanadate ions adsorption onto the mesoporous γ-AlOOH in the Na_2CrO_4–$NaAlO_2$–$NaVO_3$–H_2O solutions system of chromate production. Different from the typical impurities removing methods, without introducing Ca^{2+}, the vanadate ions were adsorbed onto the mesoporous γ-AlOOH which was synthesized by mild reaction between $NaAlO_2$ and H_2SO_4 solutions, and the obtained V(V) containing mesoporous γ-

AlOOH easily desorbed the vanadate to prepare V_2O_5 and mesoporous γ-AlOOH with high added value. Therefore, the potential applications of separation of V(V) and Al(III) from Na_2CrO_4–$NaAlO_2$–$NaVO_3$–H_2O solutions system of the chromate production and preparation of the mesoporous γ-AlOOH and V_2O_5 products with high value can be expected.

4. Conclusions

A mesoporous γ-AlOOH was synthesized by reacting $NaAlO_2$ with H_2SO_4. The synthesized mesoporous γ-AlOOH had a maximum V(V) adsorption capacity and high adsorption selectivity in the mixture solutions of V(V) and Cr(VI). The mono-oxo, V=O terminal double bonds within VO_4 units of vanadate ions were observed to connect oxygen of the coordinatively unsaturated Al^{VI} centres of the mesoporous γ-AlOOH. The mesoporous γ-AlOOH synthesis and in situ V(V) ions adsorption were used in the Na_2CrO_4–$NaAlO_2$–$NaVO_3$–H_2O solutions system of the chromate production, showing that the V(V) ions were removed effectively, so that the highly carcinogenic $CaCrO_4$ containing $Ca(VO_3)_2$ residue which obtained by typical process of chromate production could be eliminated.

Notes and references

[a] Institute of Process Engineering, Chinese Academy of Sciences, Beijing 100190, China
[b] National Engineering Laboratory for Hydrometallurgical Cleaner Production Technology, Institute of Process Engineering, Chinese Academy of Sciences, Beijing 100190, China

† Corresponding author phone: +86-10-82544808; fax: +86-10-82544808; e-mail: lipinggnipil@ipe.ac.cn

1 B. Liu, H. Du, S. Wang, Y. Zhang, S. Zheng, *AIChE J.*, 2013, **59**, 541.
2 Y. Ding, Z. Ji, in *Production and Utilization of Chromium Compounds*, ed. Chemical Industry Press, Beijing, China, 2003 (in Chinese).
3 P. R. Moskalyk, A. M. Alfantazi, *Min. Eng.*, 2003, **16**, 793.
4 S. Liao, T. Bo, in *Vanadium Metallurgy in Foreign Countries*, ed. Metallurgical Industry Press, Beijing, China, 1985 (in Chinese).
5 X. Li, C. Wei, Z. Deng, M. Li, C. Li, C. Fan, *Hydrometallurgy*, 2011, **105**, 359.
6 R. Ding, *Vanadate removal from sodium chromate solution by adding lime*; Master Dissertation, Central South University, Changsha, 2011.
7 D. M. Proctor, J. P. Panko, E. W. Liebig, P. K. Scott, K. A. Mundt, M. A. Buczynski, R. J. Barnhart, M. A. Harris, R. J. Morgan, D. J. Paustenbach, *Appl. Occup. Environ. Hyg.*, 2003, **18**, 430.
8 B. Walawska, Z. Kowalski, *J. Clean. Prod.*, 2001, 9, 219.
9 M. Claudio, E. Cristina, C. Giuseppina, M. Giuliana, *J. Chem. Soc., Faraday Trans.*, 1992, **88(3)**, 339.
10 O. Fumihiko, K. Naohito, N. Takeo, T. Seiki, *J. Colloid Interface Sci.*, 2006, **300**, 88.
11 L. Zhang, X. Jiao, D. Chen, M. Jiao, *Eur. J. Inorg. Chem.*, 2011, **2011(34)**, 5258.
12 Y. X. Zhang, Y. Jia, Z. Jin, X. Y. Yu, W. H. Xu, T. Luo, B. J. Zhu, J. H. Liu, X. J. Huang, *CrystEngComm.*, 2012, **14**, 3005.
13 S. Cabrera, J. E. Haskouri, J. A. A. Beltrán, S. Mendioroz, M. D. Marcos, P. Amorós, *Adv. Mater.*, 1999, **11**, 379.
14 C. Márquez-Alvarez, N. Žilková, J. Pérez-Pariente, J. Čejka, *Catal. Rev.*, 2008, **50**, 226.
15 D. Anirban, J. Debrina, D. Goutam, *ACS Appl. Mater. Inter.*, 2009, **4**, 833.
16 Q. H. Weng, X. B. Wang, C. Y. Zhi, Y. Bando, D. Golberg, *ACS Nano.*, 2013, **7**, 1558.
17 K. S. Sing, D. H. Everett, R. A. W. Haul, L. Moscou, R. A. Pierotti, J. Rouquerol, T. Siemieniewska, *Pure Appl. Chem.*, 1985, **57**, 603.
18 A. Naeem, P. Westerhoff, S. Mustafa, *Water Res.*, 2007, **41**, 1596.
19 X. Gong, Z. Nie, M. Qian, J. Liu, L. A. Pederson, D. T. Hobbs, N. G. McDuffie, *Ind. Eng. Chem. Res.*, 2003, **42**, 2163.
20 C. F. Baes, R. E. Mesmer, in *The hydrolysis of cations,* Wiley, New York, 1976.
21 C. Prathap, C. Namasivayam, *Environ. Chem. Lett.*, 2010, **8**, 363.
22 X. Liao, W. Tang, R. Zhou, B. Shi, *Adsorpt.*, 2008, **14**, 55.
23 F. G. Correa, J. J. Becerril, *J. Hazard. Mater.*, 2009, **162**, 1178.
24 F. Fondeur, J. L. Koenig, *J. Adhes.*, 1993, **40**, 189.
25 R. L. Frost, K. L. Erickson, M. L. Weier, O. Carmody, *Spectrochim. Acta A.*, 2005, **61**, 829.
26 I. L. Botto, M. B. Vassallo, E. J. Baran, G. Minelli, *Mater. Chem. Phys.*, 1997, **50**, 267.
27 T. W. Gregory, S. T. Oyama, A. T. Bell, *J. Phys. Chem.*, 1990, **94**, 4240.
28 J. Okal, W. Tylus, L. Kępiński, *J. Catal.*, 2004, **25**, 498.
29 J. T. Kloprogge, L. V. Duong, B. J. Wood, R. L. Frost, *J. Colloid Interface Sci.*, 2006, **296**, 572.
30 S. G. Wang, Y. Ma, Y. J. Shi, W. X. Gong, *J. Chem. Technol. Biotechnol.*, 2009, **84**, 1043.
31 Y. Arai, D. Sparks, *J. Colloid Interface Sci.*, 2001, **241**, 317.
32 T. He, L. Xiang, S. Zhu, *Langmuir*, 2008, **24**, 8284.
33 L. Luo, T. Miyazaki, A. Shibayama, W. Yen, T. Fujita, *Min. Eng.*, 2003, **16**, 665.
34 R. Navarro, J. Guaman, I. Saucedo, J. Revilla, E. Guibai, *Waste Manage.*, 2007, **27**, 425.